Proceedings of the 7th International Conference on Materials Chemistry and Environmental Engineering
DOI: 10.54254/2755-2721/2027.37744

Comparison of Aerodynamics Characters of NACA 0012 and NACA 0015

Yiting Lu

Ulink High School of Suzhou Industrial Park, Suzhou, China
Hello.Ouu@outlook.com

Abstract. This research represents a numerical analysis of the two-dimensional aerodynamics of NACA 0012 and NACA 0015 when Reynolds number is 2.2x106. Computational Fluid Dynamics(CFD) was used to perform geometric simulations, mesh generation, and graph plotting to compare the data.The results show that, in the angle-of-attack range from –5° to 5°, NACA 0015 profile, which has greater thickness, exhibits a higher drag coefficient than the NACA 0012 at the identical angle of attack, with a broader peak distribution and a more gradual recovery; at the angle of attack of 10°, the load factor curve in the trailing edge region of the NACA 0012 flattens out, indicating patterns of separation. In terms of drag, due to its greater thickness, the NACA 0015 had a higher drag coefficient than the NACA 0012 across the entire angle-of-attack range, however, the onset angle at which drag increases sharply after stall was delayed. Increased thickness enhances maximum lift and delays stall, but correspondingly increases drag. This study provides quantitative guidance for selecting wing profile thicknesses at low speeds.

Keywords: Airfoils, aerodynamic characteristics, numerical simulation

1. Introduction

Airfoil design is one of the factors that enables aircraft to generate lift. Differences in their geometric appearance determine the lift characteristics and flight safety of distinct airfoils. The NACA four-digit series is the most classic family of airfoils: its simple geometric parameters have made it a favourite among major airlines, and it has been widely used in the design and manufacture of drones, aircraft wings and underwater vehicles since the modern era. The NACA 0012 and NACA 0015 share the same maximum camber and the same relative position of the maximum camber; the distinction lies in their relative thicknesses of 12 per cent and 15 per cent, respectively. Thinner airfoils generate less drag but are vulnerable to stalling, whilst thicker airfoils produce greater lift but have lower cruising efficiency. These parameters make them ideal models for studying the influence of airfoil thickness on aerodynamic characteristics.

The angle of attack of an aerofoil is vital to its aerodynamic performance. At low angles of attack, lift increases significantly when drag remains low; as the angle of attack increases, the pressure on the aerofoil rises which leads to a sharp drop in lift. When the angle of attack exceeds a certain value, the aircraft faces the issue of stall. Consequently, understanding the effects of the angle of attack and aerofoil thickness is crucial for aerodynamic analysis.

© 2026 The Authors. This is an open access article distributed under the terms of the Creative Commons Attribution License 4.0 (https://creativecommons.org/licenses/by/4.0/).

DOI: 10.54254/2755-2721/2027.37744

In recent years, the studies on the NACA 0012 and NACA 0015 has gradually risen. Supriya Devi [1] and others employed a meshing scheme to perform a detailed, high-order curved triangular discretisation of the NACA 0012 and NACA 0015; Zhu [2] and colleagues completed a computational aerodynamic study of the FSAE tail wing airfoil; Shi and Li [3] investigated the effects of the Reynolds number on the aerodynamic performance of low-speed symmetric airfoils; and Wang [4] conducted a two-dimensional study on cavitation flow control for the NACA 0012 airfoil;Lu and Chen [5] conducted a study on the numerical simulation of aerodynamic noise near the stall angle of attack; Robiul I. Rubel et al. [6] conducted a comparative study of the aerodynamic characteristics of the NACA 0015 and NACA 4415 profiles; Touhid et al. [7] conducted a all-round performance study on the NACA 0015; research by Marwa et al. [8] and Chang et al. [9] has examined the NACA 0012 profile; James H. Page et al. [10] conducted research into pressure analysis of airfoils under specific conditions.

Under uniform calculation conditions, this paper employs CFD methods to systematically analyse the NACA 0012 and NACA 0015 airfoils at angles of attack ranging from –5° to 5°, focusing in particular on a comparison of pressure and lift coefficients, and revealing the influence of airfoil thickness on aerodynamic performance.

2. Numerical models

2.1. Geometric model

This paper selects the NACA 0012 and NACA 0015 airfoils as the subjects of numerical simulation. Figure 1 illustrates the meaning of the four-digit NACA code in a specific airfoil diagram.

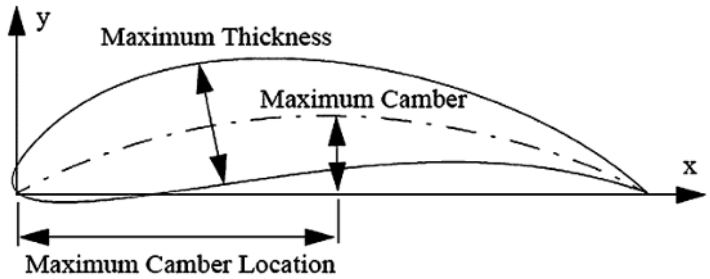


Figure 1. Explanation of airfoil parameters

Their geometric models are shown in Figures 2 and 3. Both airfoils have a maximum curvature of 0, and their maximum thickness is located at 30 per cent of the chord length.The radius of the leading edge of the NACA 0015 is correspondingly greater than that of the NACA 0012 (12 per cent), as the NACA 0015 is thicker (15 per cent).

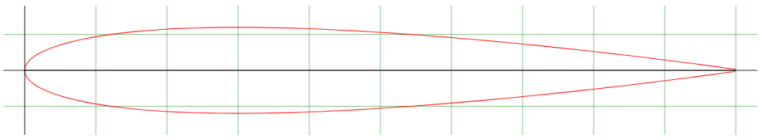


Figure 2. Diagram of the geometric appearance (NACA 0012)

DOI: 10.54254/2755-2721/2027.37744

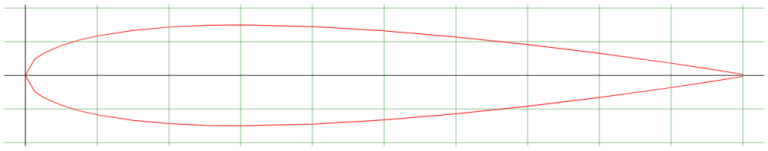
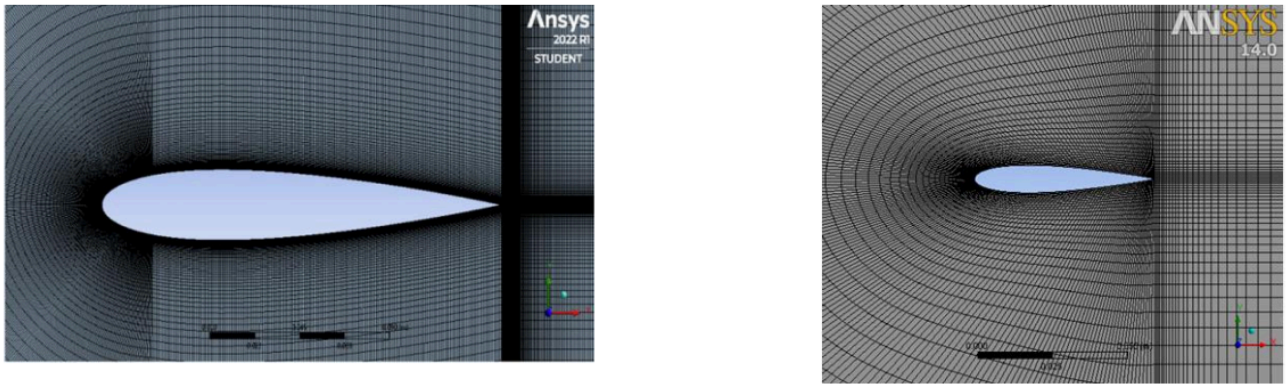


Figure 3. Diagram of the geometric appearance (NACA 0015)

2.2. Mesh division

By importing the airfoil coordinates into ANSYS Fluent, the geometric configurations of the two airfoils were obtained. The C-shaped computational domain was selected for meshing (Figure 4), with an airfoil chord length of 1 m and an inflow velocity of 32 m/s, and the Reynolds number is roughly 2.2×10^6.



(a) NACA 0012 (b) NACA 0015

Figure 4. NACA 0012 and NACA 0015 mesh generation

2.3. Boundary conditions and control equations

The medium under consideration in this simulation study is non-compressible air, and the flow satisfies the rules of conservation of mass and momentum. The continuity equation and the momentum equation are expressed as follows:

$$\frac{\partial \rho}{\partial t} + \nabla (\rho \bullet v) = 0 \tag{1}$$

$$\frac{\partial \rho}{\partial t} + \frac{\partial \rho u}{\partial x} + \frac{\partial \rho v}{\partial y} + \frac{\partial \rho w}{\partial z} = 0 \tag{2}$$

$$\rho \left(\frac{\partial (u)}{\partial t} + u\frac{\partial (u)}{\partial x} + v\frac{\partial (u)}{\partial y} + w\frac{\partial (u)}{\partial z} \right) + \frac{\partial (\rho)}{\partial x} = \mu \left(\frac{\partial^2 (u)}{\partial x^2} + \frac{\partial^2 (u)}{\partial y^2} + \frac{\partial^2 (u)}{\partial z^2} \right) \tag{3}$$

DOI: 10.54254/2755-2721/2027.37744

$$uC_p = \frac{p-p_\infty}{\frac{1}{2}\rho V^2} \tag{4}$$

In Equation (1), u represents the air velocity in the x-direction, and v represents the air velocity in the y-direction. p is the pressure, ρ denotes the density of the air, and μ represents the aerodynamic viscosity coefficient. In Equation (4), Cp is the pressure coefficient, and V represents the on-stream velocity. Table1 shows settings of conditions for this research.

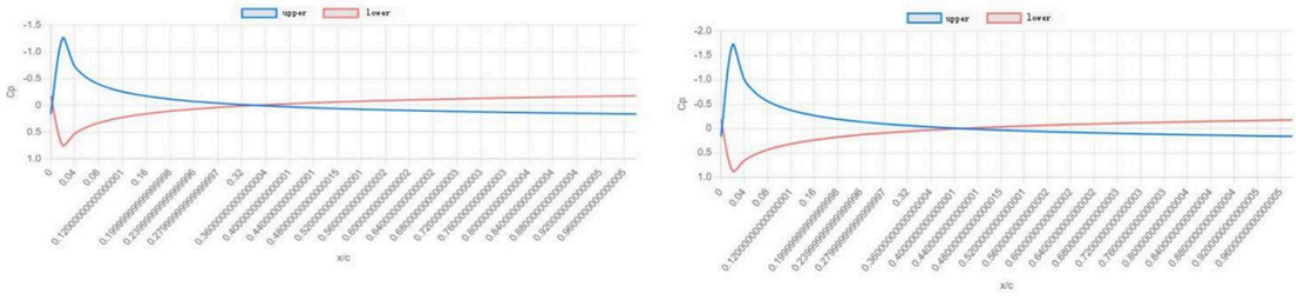
Table 1. Settings for boundary conditions

Type of solver	Pressure-Based, Steady
Air density	1.225kg/m^3
Viscosity	1.7894 x 10^$^{-5}$kg/(m-s)
Inlet velocity	32m/s
Chord length	1m
Reynolds number	2.2 x 10^^{6}
Momentum format	Second order upwind
Range of angles of attack	-5-5°

3. Results and discussion

3.1. Simulation analysis of pressure coefficients

Based on Fluent simulations, this study analyses the pressure contour plots for the NACA 0012 and NACA 0015 airfoils at angles of attack of –5°, 0°, 5° and 10°.



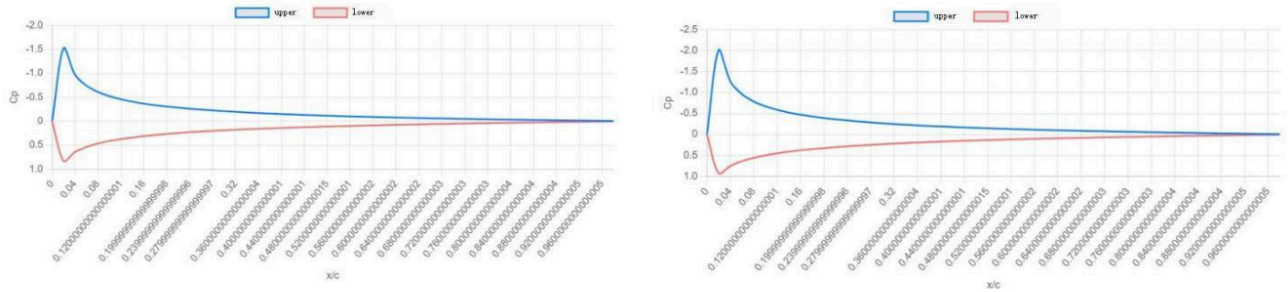
(a) NACA 0012 (b) NACA 0015

Figure 5. Pressure coefficient pattern at an angle of attack of –5°

The surface pressure of the NACA 0012 and NACA 0015 at an angle of attack of -5 degrees is shown in Figure 5. The red line shows the upper surface pressure whereas the blue line shows the lower surface pressure. Both airfoils have the same trend of pressure variation; the cp value increases quickly and reaches its maximum value at 2% of the length of the chord of the airfoil, with a difference of about 1. In the case of NACA 0012, the location where the pressure values on the

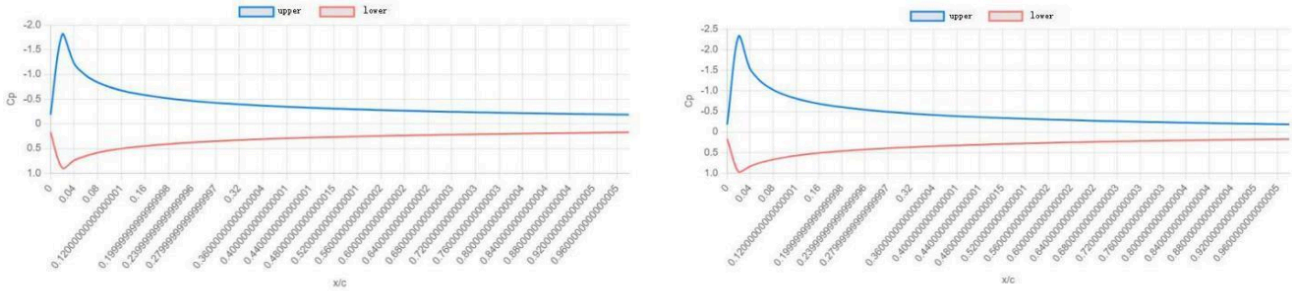
DOI: 10.54254/2755-2721/2027.37744

two surfaces are balanced is 33% of the chord length, which is about 10% smaller than in the case of NACA 0015 (44%). The distinction between the two curves of the NACA 0012 and NACA 0015 thickness is not significant, which means that thickness has a small effect on the pattern of pressure distribution at negative angles of attack. In such conditions, the actions of the upper and lower surfaces are precisely contrary to the ones at positive angles.



(a) NACA 0012 (b) NACA 0015

Figure 6. Pressure coefficient pattern at an angle of attack of 0°



(a) NACA 0012 (b) NACA 0015

Figure 7. Pressure coefficient pattern at an angle of attack of 5°

The distribution of surface pressure coefficients of the two airfoil profiles at a 0 angle of attack are presented in Figures 6 and 7. The Cp curves for the upper and lower surfaces of both airfoil profiles coincide exactly; the blue and red lines overlap, and the total lift is zero. Figures7 compares the pressure distributions of the two airfoil profiles at a 5 angle of attack. The suction peaks on the upper surfaces of the two airfoils are measured at 2 percent, the suction peak of the NACA 0015 is less (10%) and has a larger span compared to the NACA 0012, which implies that the thicker airfoil accelerates better at the leading edge; at the same time, the pressure values of the lower surface (red) grow. The amount of separation between the curves of the two airfoils is about the same; the area below the NACA 0015 curve is a bit larger than the NACA 0012 curve, which means it produces a slightly higher lift at the same angle.

3.2. Comparative analysis of drag coefficients

The figures produced by Shi and Li [3] show the change in drag values across the NACA 0012 and NACA 0015 airfoils under various attack angles. The line where the diamond is placed indicates the

DOI: 10.54254/2755-2721/2027.37744

calculated value of pressure; the triangle is the test value of the pressure; the square is the calculated value of resistance, and the cross is the test value of resistance. At angles of attack between 0-12°the drag coefficient of each airfoil increases steadily with increasing angle. At this stage, the flow over both airfoils is completely attached and experimental values are only slightly different compared to the CFD calculation results. The NACA 0015 has a greater drag coefficient than NACA 0012, but this difference is essentially the same throughout the range of angles. Because it is thicker and has a greater wing-section area, the NACA 0015 has higher frictional drag than the NACA 0012. This is the intrinsic aerodynamic penalty of high thickness. In the two line plots shown, the diamonds stand for calculated pressure readings and the triangles stand for experimental readings; the squares indicate calculated resistance values and the crosses indicate experimental values.

For the NACA 0012, the Cd value begins to increase sharply at approximately 16°, whilst for the NACA 0015, the angle at which the Cd begins to increase sharply is delayed by approximately 2°compared to the NACA 0012, resulting in a stall condition. When the angle exceeds 16°, the Cd of both airfoils increases significantly. Although the absolute drag value of the NACA 0015 may be higher, it exhibits greater lift-maintaining capability; at the same attack angle, the lift-drag ratio decreases more gradually than that of NACA 0012. During this phase, the calculated drag values are significantly lower than the experimental values.

4. Conclusion

This research comprehensively investigates and compares the aerodynamic characteristics of NACA 0012 and NACA 0015 using CFD. The comparison of the flight performance and the surface pressure distribution in an angle of attack range of -5°to 5°was performed and the outcomes were graphed. Conclusions to be drawn based on this research are:

Both airfoils have linear variations in their pressure coefficients in the angle-of-attack range of -5°to 5°. The NACA 0015 has a higher pressure coefficient than the NACA 0012 at the same angle of attack, because it has a thicker wall, and this difference is amplified with increasing angle of attack.

At low angles of attack (0-15°) in the linear region, both airfoils have an increasing drag that follows lift, and the NACA 0015 is always a little higher than the NACA 0012. After the start of stall, the pressure-difference drag of both airfoils rises significantly; nonetheless, the angle of attack at which NACA 0015 has drag surge is about 3 degrees below the same angle of attack where NACA 0012 achieves its surge.

The peak value for NACA 0015 is more negative and has a broader distribution than that of NACA 0012, indicating that the leading edge of the thicker airfoil accelerates more fully, which explains why the increased thickness delays the onset of stall.

References

[1] Supriya, D., Nagaraja, K. V., Smitha, T. V., & Jayan, S. (2019). Accurate higher order automated unstructured triangular meshes for airfoil designs in aerospace applications using parabolic arcs. Aerospace Science and Technology, 88, 405-420.

[2] Wei Fengqi, Bai Yuxing, Zhu Jiahui, Zhao Yingru & Zang Liguo. (2024). Aerodynamic Study of FSAE Tail Fin Airfoils. Mechanical Engineer, (11), 61–65.

[3] Shi Guangtai & Li Zhenpeng. (2013). The Effect of the Reynolds Number on the Aerodynamic Performance of Low-Speed Symmetrical Airfoils. New Technologies and New Processes, (9), 18–22.

[4] Wang Weijun. (2022). A Study on the Control of Cavitation Flow around a NACA0012 Two-Dimensional Airfoil. Journal of Wuhan University (Engineering Edition), 55(5), 525–530.

DOI: 10.54254/2755-2721/2027.37744

[5] Lu Qinghua & Chen Bao. (2014). A Numerical Simulation Study of Aerodynamic Noise of the NACA0012 Airfoil Near the Stall Angle of Attack. In (eds.) Exploration, Innovation, Exchange: Proceedings of the 6th China Aeronautical Society Young Scientists and Engineers Forum (Volume 1) (pp. 235–241). Aerodynamics Research Institute, AVIC

[6] Rubel, R. I., Uddin, M. K., Islam, M. Z., & Rokunuzzaman, M. (2016). Comparison of Aerodynamics Characteristics of NACA 0015 & NACA 4415.

[7] Orvi, T. A., Hossain, I., & Hassan, M. (2025). Computational and experimental investigation of lower-surface dimple effects on NACA 0015 airfoil aerodynamics. Engineering Science and Technology, an International Journal, 72, 102228.

[8] Rashid, M. K., Abed, K. N., Alharbi, M., Muayad, M. W., Alkharusi, T., & Ameen, A. (2025). Integrating machine learning and CFD for enhanced trailing edge serration design on a NACA 0012 wind turbine blade. International Journal of Thermofluids, 101446.

[9] Chang, J., Zhang, Q., He, L., & Zhou, Y. (2022). Shedding vortex characteristics analysis of NACA 0012 airfoil at low Reynolds numbers. Energy Reports, 8, 156-174.

[10] Page, J. H., Ozcer, I., Zanon, A., De Gennaro, M., & Llamas-Sandin, R. C. (2025). Aerodynamics and ice tolerance of the large passenger aircraft advanced rear end forward swept horizontal tailplane with leading edge extension. Aerospace Science and Technology, 161, 110018.